Article

ACS AuthorChoice

Enhanced Acidity of Acetic and Pyruvic Acids on the Surface of Water

Alexis J. Eugene,[†] Elizabeth A. Pillar,[†] Agustín J. Colussi,[‡] and Marcelo I. Guzman*,[†]

[†]Department of Chemistry, University of Kentucky, Lexington, Kentucky 40506, United States
[‡]Department of Environmental Science & Engineering, California Institute of Technology, Pasadena, California 91125, United States

ABSTRACT: Understanding the acid−base behavior of carboxylic acids on aqueous interfaces is a fundamental issue in nature. Surface processes involving carboxylic acids such as acetic and pyruvic acids play roles in (1) the transport of nutrients through cell membranes, (2) the cycling of metabolites relevant to the origin of life, and (3) the photooxidative processing of biogenic and anthropogenic emissions in aerosols and atmospheric waters. Here, we report that 50% of gaseous acetic acid and pyruvic acid molecules transfer a proton to the surface of water at pH 2.8 and 1.8 units lower than their respective acidity constants $pK_a = 4.6$ and 2.4 in bulk water. These findings provide key insights into the relative Bronsted acidities of common carboxylic acids versus interfacial water. In addition, the work estimates the reactive uptake coefficient of gaseous pyruvic acid by water to be $\gamma_{PA} = 0.06$. This work is useful to interpret the interfacial behavior of pyruvic acid under low water activity conditions, typically found in haze aerosols, clouds, and fog waters.
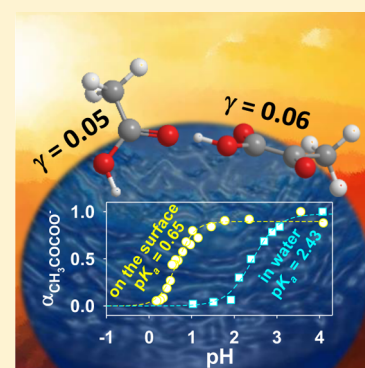
■ INTRODUCTION

The study of dissociation constants (K_a) at interfaces has been the goal of recent experimental and theoretical works.[1,2] Surface sensitive measurements by online electrospray ionization mass spectrometry (OESI-MS) for hexanoic acid and theoretical calculations combined with molecular dynamics simulations for pyruvic acid show a drop in their $pK_a = -\log K_a$ on the surface of water.[1,2] OESI-MS reveals signals for the fast collision of gaseous organic acids on the surface of water, sampling pK_a values of the nanometric interface layer that are independent of the behavior of bulk molecules.[1] A major challenge for this kind of experiment is to quantify the shift in pK_a upon adsorption of the gaseous carboxylic acid on the surface of water. OESI-MS should not be confused with the traditional configuration of electrospray ionization mass spectrometry (ESI-MS) that only samples bulk phase composition. Infused solutions into an ESI-MS configuration show pK_a values of hexanoic and octanoic acids in bulk water, which agree well with long-established titration techniques.[3] Similarly, surface tension titrations of millimolar concentrations of octanoic acid display a pK_a value identical to the accepted bulk value.[4]

Understanding the behavior of carboxylic acids, such as acetic and pyruvic acids, on the surface of water is a fundamental chemical problem with biochemical, prebiotic chemistry, and environmental implications. For example, the biochemical uptake of pyruvic acid by cells is mediated by a transporter, bringing pyruvate across the membrane.[5] Also of interest are prebiotic chemical cycles that use pyruvic acid as a central metabolite in interfacial reactions related to the origin of life.[6−9] In addition, pyruvic acid is abundant in tropospheric aerosols[10−12] because of the atmospheric photooxidative processing of biogenic and anthropogenic emissions.[13−15] As a chromophore, pyruvic acid is one of the few carboxylic acids in the atmosphere that can undergo solar photochemistry in the aqueous phase.[16−21] Thus, the transfer of gaseous pyruvic acid to the aqueous phase, with a large Henry's law constant ($K_H = 3.1$ mol kg^{-1} Pa^{-1}),[22] is of particular atmospheric interest. The C=O group of pyruvic acid ($pK_a = 2.39$ in bulk water)[23] undergoes cooperative reversible hydration (with equilibrium constant $K_{Hyd} = 1.83$) into 2,2-dihydroxypropanoic acid, an ultraviolet transparent gem-diol.[24]

The complexity of considering the orientation of pyruvic acid within the accommodation process on the surface of water and the effect of pH on photoreactivity changes[25,26] demand a better understanding of the acid−base properties that pyruvic acid senses and exerts at the air−water interface. In addition, to the best of our knowledge, there is no literature available reporting the reactive uptake coefficient of gaseous pyruvic acid by water (γ_{PA}). Thus, this work uses a customized OESI-MS setup to study the acid dissociation constants of acetic and pyruvic acids. The Bronsted basicity of the air−water interface has been characterized by OESI-MS in a different setup.[1] Herein, we contrast the pK_a of acetic or pyruvic acids in water by ESI-MS with those measured by OESI-MS on the surface of pH-adjusted microdroplets impinged by gas-phase molecules of the acids. Using reliable parameters for acetic acid and the present measurements allows the estimation of γ_{PA}.

MATERIALS AND METHODS

Sample Preparation for Experiments in Water. Aqueous solutions were prepared from pyruvic acid (Sigma-Aldrich, 98.5%, distilled under vacuum) and acetic acid (glacial, ≥99.7%, Acros) with formula masses of 88.06 and 60.05 Da, respectively. All solutions were prepared in ultrapure water (Elga PURELAB flex, 18.2 MΩ cm^{-1}). Sodium hydroxide (NaOH, Acros, 0.1 N) and hydrochloric acid (HCl, EMD, 12.1 M) were used to prepare stock solutions for pH adjustment. The dropwise addition of HCl and NaOH solutions was performed under continuous stirring with burets (Kimble KIMAX, Class A) and measured with a calibrated pH-meter (Mettler Toledo). Throughout, the pH values reported herein are the pH values measured in the bulk solutions prior to infusion into the nebulizing chamber. Because pH represents chemical potential, all phases in equilibrium, viz. interfacial and bulk water, must have the same pH.

Sample Preparation for Experiments on the Surface of Water. Pyruvic acid solution (1.43 M) in water held at 25.0 °C in a wash bottle for gases and immersed in a chiller bath (Thermo Scientific A25) was sparged with 0.10 L min^{-1} flow of N$_2$(g). The gas carrying pyruvic acid was then mixed with 0.10 L min^{-1} flow of N$_2$(g) using a custom-built gas proportioner. After dilution, the total flow of 0.20 L min^{-1} was transported through a stainless steel tube to the aerosolization chamber. Similarly, a 1.00 M acetic acid solution in water or cyclohexanol (J.T. Baker, 100%) was held in the wash bottle for gases at 17.0 °C and sparged with 0.020 L min^{-1} flow of N$_2$(g). The gas carrying acetic acid was then diluted with 2.150 L min^{-1} flow of N$_2$(g) using a gas proportioner. A common inlet flowmeter was used to divert only 0.20 L min^{-1} of the diluted acetic acid into the aerosolization chamber.

Instrumental Conditions. The conditions for ESI-MS and OESI-MS measurements were set to a nebulizer voltage of −2.2 kV, a cone voltage of 40 V, and a nebulizer pressure of 70 psi N$_2$(g). The only difference was the drying gas temperature of 350 °C in ESI-MS and 50 °C in OESI-MS. All reported titration curves were built by plotting normalized I_{59} and I_{87} values for the anions CH$_3$COO$^-$ and CH$_3$COCOO$^-$ of acetic and pyruvic acids, respectively, versus the measured bulk pH of the solution from which the droplets were formed. The largest registered ion count in each set of experiments was arbitrarily assigned unity value and was used to normalize all other $I_{m/z}$ values at variable pH. The mass spectrum of each sample was acquired at fixed time intervals (e.g., time ≥ 1 min).

ESI-MS. Solutions were pumped at 50 µL min^{-1} into the pneumatically assisted ESI interface coupled to a single quadrupole MS (Thermo Scientific MSQ Plus) described in detail before.[27] For experiments "in" water, the solutions of acetic and pyruvic acids at the adjusted pH were directly infused for single-ion monitoring in the negative ionization mode, registering the ion count ($I_{m/z}$) at the mass-to-charge ratios (m/z) of 59 and 87, respectively.

OESI-MS. For experiments "on" the surface of water, the 0.20 L min^{-1} flow of N$_2$(g) carrying carboxylic acid was directed via an electrically grounded stainless steel tube to collide with the generated microdroplets.[28,29] For the production of microdroplets, solutions were pumped at 50 µL min^{-1} into the same electrospray probe of the MSQ Plus instrument mentioned above. The gas-phase molecules impinging the microdroplets during a contact time τ_c = 1 µs generate signals that sense the interface of water.[28,29] In this setup, the exhaust of the gas mixture was positioned 32 mm away from the entrance cone and 12 mm from the needle tip carrying the solution. Furthermore, a final 61-times dilution with the N$_2$(g) nebulizing gas (12.0 L min^{-1}) occurred in this chamber.[29] The fact that the same products are identified after offline analysis of surface reactions lasting a few hours and in situ studies under a few microseconds of contact time validates the OESI-MS setup for probing reactions at the air–water interface.[28,30]

The temperature-dependent vapor pressure of the acids[31] was used to calculate the final mixing ratios of 2.00 and 1.40 ppmv for acetic and pyruvic acids, respectively. These final mixing ratios are the ones encountered by the surface of continuously generated aqueous microdroplets of adjusted pH. The gas-phase molecules of acetic or pyruvic acid accommodate on the surface of the microdroplets prepared at fixed pH values, which were measured with the calibrated pH-meter. Deprotonation proceeds only during this encounter with the first generation of microdroplets that conserve the measured bulk pH. Immediately following the deprotonation, the cascade breakup of the particles forming the ions proceeds with the help of the desolvation gas. These ions are detected by a mass spectrometer within 1 ms in the negative ionization mode.

RESULTS AND DISCUSSION

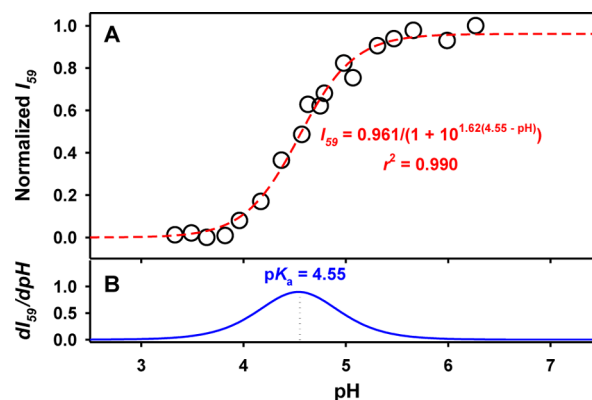**Experiments "in" Water Solution.** Figure 1 displays the titration curve for acetic acid in water determined by ESI-MS

Figure 1. (A) ESI-MS titration curve for 100 µM acetic acid in water. (○)Normalized ion count for the acetate anion at m/z 59, I_{59}, as a function of pH fitted with a (red line) sigmoid curve with the coefficient of correlation r^2 = 0.990. (B) First derivative of the sigmoid curve in (A), where the maximum corresponds to pK_a (blue line).

in a typical experiment. Considering the Henderson–Hasselbalch equation, I_{59} values are directly proportional (∝) to the measured dissociation fraction of acetate in Figure 1

$$\alpha_{CH_3COO^-} = \left(\frac{[CH_3COO^-]}{[CH_3COO^-] + [CH_3COOH]} \right) \propto I_{59} \quad (1)$$

The dissociation fraction of acetate (and the representative normalized I_{59} value) spans from $\alpha_{CH_3COO^-}$ = 0 for the bulk solution with only undissociated acid up to $\alpha_{CH_3COO^-}$ = 1 when only the conjugate base is present. The inflection point of the characteristic sigmoid curve fitting the dataset in Figure 1 marks pK_a, which indicates at which bulk acid strength the concentrations of the acid and base forms are equal. More specifically, the inflection point is located at $I_{59} \cong \alpha_{CH_3COO^-}$ = 0.5, where pH = pK_a = 4.55 and the asymptote tends to 1.

The titration curve for pyruvic acid in water obtained by ESI-MS is presented in Figure 2. The normalized I_{87} values are also directly proportional to the measured dissociation fractions of pyruvate at variable pH in Figure 2

$$\alpha_{CH_3COCOO^-} = \left(\frac{[CH_3COCOO^-]}{[CH_3COCOO^-] + [CH_3COCOOH]} \right) \propto I_{87} \quad (2)$$

As explained above for the case of acetate, the normalized dissociation fraction of pyruvate is also limited to the range 0 ≤ $\alpha_{CH_3COCOO^-}$ ≤ 1. The inflection point for pyruvic acid in water is located at $I_{87} \cong \alpha_{CH_3COCOO^-}$ = 0.5, where pH = pK_a = 2.43 (Figure 2).
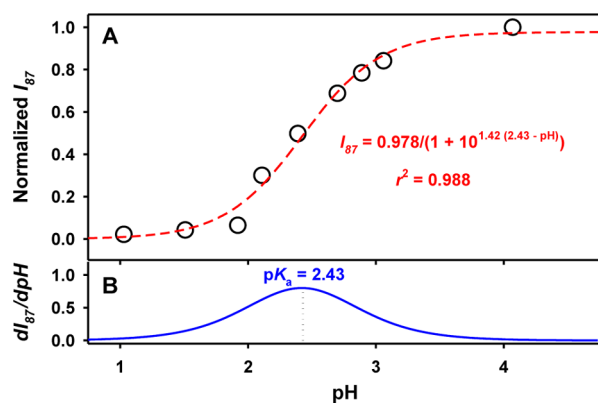
Figure 2. (A) ESI-MS titration curve for 100 μM pyruvic acid in water. (○)Normalized ion count for the pyruvate anion at m/z 87, I_{87}, as a function of pH fitted with a (red line) sigmoid curve with the coefficient of correlation $r^2 = 0.988$. (B)First derivative of the sigmoid curve in (A), where the maximum corresponds to the pK_a (blue line).

The nonlinear fittings in Figures 1 and 2 with correlations $r^2 \geq 0.98$ allow the determination of the pK_a values by reproducing the titration curves of acetic and pyruvic acids in bulk solutions with <5.0% error relative to respective literature values of 4.75 and 2.39.[23] Any deviations from the literature pK_a values, possibly due to electric fields on the surface of water,[32] are therefore negligible and can be disregarded. This statement is corroborated by the fact that *both* gas-phase bases (like trimethylamine) *and* acids are protonated and deprotonated on the surface of water at pH values lower than their pK_a's in bulk water. Electric fields do not perturb the charge balance of the double layer; otherwise, they should have had opposite effects on the titration of acids and bases on the surface of water.[1,3] Therefore, this procedure is valid for determining the pK_a values of low-molecular-weight carboxylic acids, in agreement with previous observations made for *n*-hexanoic and *n*-octanoic acids with a different ESI-MS setup.[3] Thus, the measured pK_a values imply that standard eqs 3 and 4 also govern the deprotonation behavior registered for acetic and pyruvic acids, respectively[3]

$$\alpha_{CH_3COO^-} = \frac{1}{1 + 10^{m_{CH_3COOH}(pK_a^{CH_3COOH} - pH)}} \quad (3)$$

$$\alpha_{CH_3COCOO^-} = \frac{1}{1 + 10^{m_{CH_3COCOOH}(pK_a^{CH_3COCOOH} - pH)}} \quad (4)$$

where m_{CH_3COOH} and $m_{CH_3COCOOH}$ are the slopes of the respective sigmoid curves, which take unity value in traditional titration methods, and the dissociation fractions clearly depend on the difference (pK_a − pH) rather than only on pH. Therefore, the observed titration curves reflect functions in which neither pK_a nor pH has practically shifted relative to their bulk values.[3] Thus, it can be deduced that the pH of the experiments in Figures 1 and 2 cannot be distinguished from those in bulk solution.

Experiments "on" the Surface of Water. Figure 3 shows the results for a typical OESI-MS experiment detecting acetate generated from the dissociation of gaseous acetic acid deposited on the surface of water adjusted to variable pH with HCl and NaOH. In this case, acetic acid is carried out by a flow of $N_2(g)$ from an aqueous solution before it collides on the surface of the aqueous microdroplets. The inflection point for the sigmoid fitting of Figure 3A, matching the maxima for
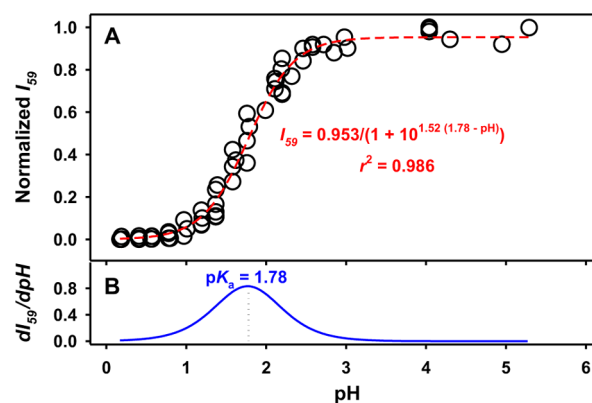

Figure 3. (A) OESI-MS titration curve for acetic acid (from a solution in water) deposited on the surface of water for microdroplets exposed to 2.00 ppmv ($\equiv 4.55 \times 10^{13}$ molecules cm^{-3} under the experimental conditions) for a contact time $\tau_c = 1$ μs. (○)Normalized ion count for the acetate anion at m/z 59, I_{59}, as a function of pH fitted with a (red line) sigmoid curve with the coefficient of correlation $r^2 = 0.986$. (B) First derivative of the sigmoid curve in (A), where the maximum corresponds to pK_a (blue line).

its first derivative in Figure 3B, indicates p$K_a = 1.78$ for gaseous acetic acid deposited on the surface of water.

Figure 4 displays the OESI-MS titration curve for gaseous acetic acid sparged on the surface of water after it was carried
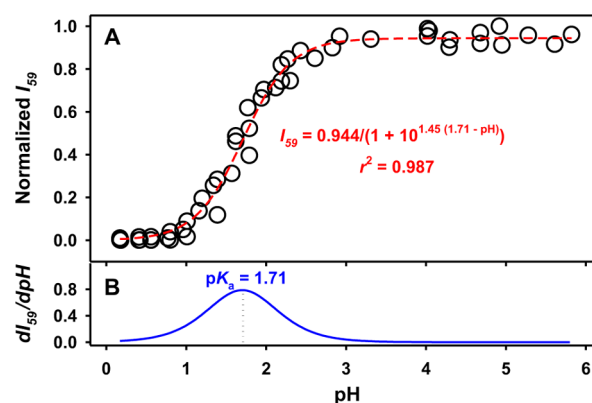

Figure 4. (A) OESI-MS titration curve for acetic acid (from a solution in cyclohexanol) deposited on the surface of water for microdroplets exposed to 2.00 ppmv ($\equiv 4.55 \times 10^{13}$ molecules cm^{-3} under the experimental conditions) for a contact time $\tau_c = 1$ μs. (○)Normalized ion count for the acetate anion at m/z 59, I_{59}, as a function of pH fitted with a (red line) sigmoid curve with the coefficient of correlation $r^2 = 0.987$. (B) First derivative of the sigmoid curve in (A), where the maximum corresponds to the pK_a (blue line).

out from a solution in cyclohexanol by a flow of $N_2(g)$. This experiment using cyclohexanol discards that water vapor carried with the stream of carboxylic acid has any effect on the measured pK_a. The experiment in Figure 4 shows p$K_a = 1.71$, which is only 3.9% different from that determined using water as the starting solvent (Figure 3). The key finding here is that the measured pK_a for CH$_3$COOH(g) deposited on the surface of water (Figures 3 and 4) drops 2.75 ($\pm$0.05) pH units relative to CH$_3$COOH(aq) in bulk water (Figure 1). By contrasting the results in Figure 1 with those in Figures 3 and 4, it is evident that CH$_3$COOH(g) on the air side of the interface behaves as a 590-times stronger Bronsted acid than CH$_3$COOH(aq) on the water side of the interface under the

same bulk pH. In addition, these results confirm that the detection of I_{59} corresponds to acetate ions that have not yet dissolved in the bulk of the microdroplets but that are produced from the air side of the interface. Otherwise, there should be no difference in the pK_a values of the titrations in Figure 1 from those in Figures 3 and 4.

The experiments in Figures 3 and 4 employed a high mixing ratio of 2.00 ppmv $CH_3COOH(g)$, which is larger than the maximum 300 ppbv ($\equiv 7.39 \times 10^{12}$ molecules cm^{-3}) of organic acid needed to reach the plateau for Langmuir adsorption in this kind of system.[1] Therefore, the available water surface of generated microdroplets is fully covered by impinging acetic acid molecules. Under these conditions, it is clear that gaseous acetic acid does not transfer its proton to neutral water molecules directly but to the interfacial dangling basic groups,[33] $HO^-_{interface}$, which limit the amount of CH_3COO^- ions generated and detected. The surface density of $HO^-_{interface}$ toward the air side of the aqueous microdroplet interface, $S_{HO^-_{interface}}$, available to interact with $CH_3COOH(g)$ molecules can be estimated from the product of two terms, the frequency of collisions provided by the kinetics theory of gases and $\tau_c = 1$ μs

$$S_{HO^-_{interface}} = \frac{\gamma_{AA} v_{AA} n}{4} \times \tau_c \tag{5}$$

where the reactive uptake coefficient for acetic acid is $\gamma_{AA} = 0.05$,[34] the mean thermal velocity of gaseous acetic acid at 298 K is $v_{AA} = 3.52 \times 10^4$ cm s^{-1}, and the number density for 300 ppbv acetic acid is $n = 7.39 \times 10^{12}$ molecules cm^{-3}. By the substitution of the previous values in eq 5, an estimate of $S_{HO^-_{interface}} = 3.25 \times 10^9$ HO^- cm^{-2} is obtained for the experiments in Figures 3 and 4, which is equivalent to a surface charge density $q = 0.52$ nC cm^{-2}. The reported $S_{HO^-_{interface}}$ and its associated q value in our aqueous microdroplet setup are in excellent agreement with those reported from experiments with hexanoic acid sparged on the surface of a water jet during 10 μs contact time.[1] Previous work has demonstrated that anions can populate the interface of water with air at depths that are inversely proportional to the square of their size, as represented by the ionic radius, even for dissimilar concentrations affecting the sublayers.[27,35,36] Thus, the fact that q is 2×10^3 times smaller than that observed from ζ-potential measurements in the electrophoresis of bubbles and oil droplets in water[33,37] is logically explained as reflecting experiments that have tested the basicity of water at different depths.[1]

When a gas stream of pyruvic acid, generated by a flow of $N_2(g)$ through a solution in water, encounters the interface of the pH-adjusted aqueous microdroplets, pyruvate is immediately formed by dissociation (Figure 5). The sigmoid fitting of Figure 5A for gaseous pyruvic acid deposited on the surface of water at variable pH has an inflection point at $pK_a = 0.65$ matching the maxima for its first derivative in Figure 5B. By comparison, the measured pK_a for $CH_3COCOOH(g)$ deposited on the surface of water (Figure 5) drops 1.78 pH units relative to $CH_3COCOOH(aq)$ in bulk water (Figure 2). Thus, the air side of the interface senses $CH_3COCOOH(g)$ to be 55-times stronger as a Bronsted acid than $CH_3COCOOH(aq)$ on the water side of the interface.

The high number of $[CH_3COCOOH(g)] = 3.28 \times 10^{13}$ molecules cm^{-3} in the experiment of Figure 5 also exceeds the expected plateau for Langmuir adsorption of low-molecular-
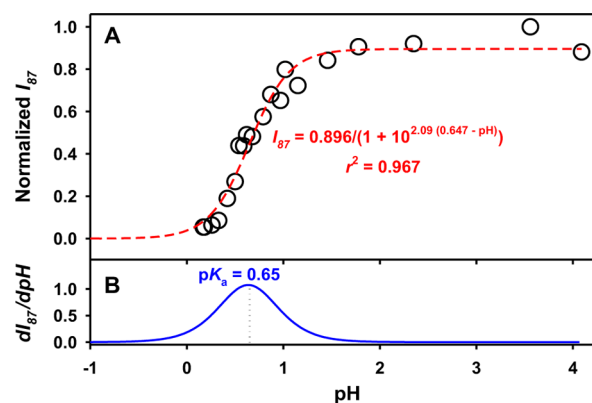

Figure 5. (A) OESI-MS titration curve for pyruvic acid (from a solution in water) deposited on the surface of water for microdroplets exposed to 1.40 ppmv ($\equiv 3.28 \times 10^{13}$ molecules cm^{-3} under the experimental conditions) for a contact time $\tau_c = 1$ μs. (○)Normalized ion count for the acetate anion at m/z 87, I_{87}, as a function of pH fitted with a (red line) sigmoid curve with the coefficient of correlation $r^2 = 0.967$. (B) First derivative of the sigmoid curve in (A), where the maximum corresponds to the pK_a (blue line).

weight carboxylic acids.[1] A reasonable estimate for the reactive uptake coefficient of gaseous pyruvic acid by water of $\gamma_{PA} = 0.06$ can be retrieved after rearranging eq 5 for this molecule as follows

$$\gamma_{PA} = \frac{4 S_{HO^-_{interface}}}{v_{PA} n \tau_c} \tag{6}$$

where the mean thermal velocity used is that of $CH_3COCOOH(g)$ at 298 K, $v_{PA} = 2.91 \times 10^4$ cm s^{-1}, $n = 7.39 \times 10^{12}$ molecules cm^{-3},[1] and $\tau_c = 1 \times 10^{-6}$ s for this system,[29] and the value $S_{HO^-_{interface}} = 3.25 \times 10^9$ HO^- cm^{-2} is obtained above using acetic acid.

It is important to highlight that before this study, only one experimental report had tackled the investigation of pK_a shifts by observing a transfer of protons initiated from the air side of the air−water interface.[1] It should be emphasized that Bronsted acidity and basicity are relative concepts that describe the extent of proton transfer of acids and bases with the local solvent. Herein, we demonstrate that the surface of water is more basic than the bulk, meaning that it is a better proton acceptor than bulk water. Vibrational sum frequency spectroscopy (VSFS) experiments on interfaces of aqueous solutions of acetic acid (of unreported pH) revealed the sole presence of undissociated acid,[38] even at the lowest acid concentrations, which exceeded those used in our experiments by a factor of 3. VSFS experiments were apparently unable to detect acetate,[38] possibly due to limitations on the alignment of moieties at the interface.[39] Furthermore, we wish to point out the absence of VSFS experiments on acetate solutions.[38] We consider that VSFS data are moot regarding the extent of dissociation of acetic acid on the surface of its aqueous solutions.[38] In short, acidity is a property that depends on the medium and is defined by the local equilibrium constant for the process AH + $H_2O \rightleftharpoons A^- + H_3O^+$. This equilibrium may have different pK_a values on the surface versus in the bulk because the acid and water may have different acid−base properties as a result of the differential hydration of reactants and products, as discussed in the next section.

Dependence of the pK_a Shifts on the Selective Hydration of Acid−Base Pairs. The pK_a shift of 2.75

units from the bulk phase to the surface of water for acetic acid agrees well with the observations for hexanoic and octanoic acids.[1,3] Similar to simple monocarboxylic acids, the impinging gaseous acetic acid molecule has its −COOH group oriented in an upright position with respect to the surface.[40] In other words, when gaseous acetic acid reaches the local plane of the interface, its −COOH group points to the aqueous core with the plane established by the −COOH group with a C_{sp^2} oriented perpendicularly to the surface plane. Simultaneously, the hydrophobic −CH₃ of acetic acid is repelled into the air, aligning the axis defined by the C−C bond close to the surface normal (with a tilt ≤15° from the surface normal).[40] A similar assumption could be made for the corresponding −COO⁻ group[41] from quickly formed acetate after proton loss from the acid form that has accommodated at the interface.
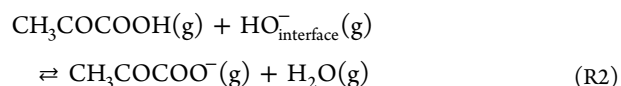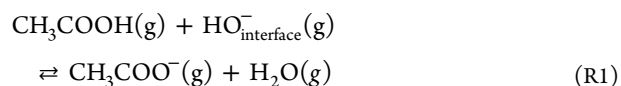
Additional water molecules can contribute to hydrating the −COO⁻ group formed at the interface, changing the amphiphilic balance of the molecule.[42] On this basis, photoelectron spectroscopy and VSFS measurements have proposed that enrichment of acetic acid relative to acetate occurs at the interface.[38,42] However, we interpret the previous spectroscopy studies of acetic acid solutions to have sampled the interior layer of the interface of acetic acid solutions. Instead, in our work, the external layers of the interface are directly sampled, as gaseous acetic acid collides with water, showing that the acid has a larger capacity to transfer its proton to surface water (that behaves as a base) than in the bulk. Therefore, acetic acid behaves as a stronger acid at the interface, and the ratio [−COO⁻]/[−COOH] sensed from the air side of the air−water interface is larger than in the bulk. In other words, the interfacial ratio [−COO⁻]/[−COOH] cannot be predicted by bulk pK$_a$ values.

For pyruvic acid, a smaller pK$_a$ shift of 1.78 units is observed, which is in agreement with the shift of 1.84 pK$_a$ units computed at the quartz−water interface using a combination of ab initio molecular dynamics simulations.[2] Whereas the likelihood of natural hydrophobic quartz surfaces is low (covered with siloxane Si−O−Si bridges), Parashar et al. modeled the most common hydrophilic quartz surface with −OH groups from the silanols[43] directly in contact with water.[2] Because the orientation of pyruvic acid at the air−water interface remains unexplored, the quartz−water model serves here as a first-order approximation for visualizing the behavior of the hydrophilic −OH groups from the terminal silanols in contact with water. Related VSFS measurements show that the interfacial potential at the quartz−water and air−water interfaces for the surface adsorption of lysozyme is controlled by the protonation/deprotonation of the protein's groups.[39] Whereas at the air−water interface, some lysozyme residues are organized at the hydrophobic air surface, major changes are only observed on the hydrophilic quartz−water interface for pH > 8.0, when a net negative charge is developed.[39] Therefore, such an extrapolation of the interfaces provides an initial model to interpret the mechanism by which gaseous pyruvic acid interacts with the surface of water under the experimental pH conditions explored in Figure 5.

At variance with the perpendicular geometry for acetic acid, the −COOH group of pyruvic acid is pictured to be practically plane parallel to the surface of water (as shown in the table of content graphic). Remarkably, radial distribution functions for pyruvic acid and pyruvate with the oxygen and hydrogen atoms of water, respectively,[2] suggest that the acid remains localized, with C=O accommodated on the surface of water while

getting hydrated.[24] The previous configuration constrains the hydrophobic −CH₃ group of the acid to be in contact with the surface of water. Therefore, the different surface propensity of pyruvic acid relative to acetic acid also affects the interfacial abundance of each acid−base pair.[42] Pyruvate also plays an important role favoring the dissociation of pyruvic acid at the interface. On the surface, pyruvate not only forms hydrogen bonds with water from the first monolayer, but as it gets buried deeper than the neutral molecule, it also gains additional stabilization by H bonds with the contiguous layer of water.[2] Thus, the enhanced acidity of pyruvic acid at the interface is ascribed to the differential microsolvation of the acid versus its conjugated base. The pK$_a$ shift is associated with the molecular orientation of pyruvic acid/pyruvate at the air−water interface as well as the local structure and proton-accepting properties of interfacial water.[2]

The results presented in the previous section for gaseous acetic and pyruvic acids follow the thermodynamically favorable interfacial proton transfer behavior[1] dictated by reactions R1 and R2 with dissociation constants $K_{a,R1} = 1.78 \times 10^{-2}$ and $K_{a,R2} = 2.24 \times 10^{-1}$, respectively:

$$CH_3COOH(g) + HO^-_{interface}(g)$$
$$\rightleftarrows CH_3COO^-(g) + H_2O(g) \tag{R1}$$

$$CH_3COCOOH(g) + HO^-_{interface}(g)$$
$$\rightleftarrows CH_3COCOO^-(g) + H_2O(g) \tag{R2}$$

In the surface process studied here, increased dissociation constants are observed for both acids relative to bulk water. An alternative explanation to the smaller acidity shift displayed by pyruvic acid involves an assessment of the larger net water cluster containing the $HO^-_{interface}$ that participates in reaction R2 relative to R1. Comparing the results for both acids on the surface of water (Figure 5 vs Figures 3 and 4) indicates that the experimentally determined ratio $K_{a,R2}/K_{a,R1} = 12.44$

$$\frac{K_{a,R2}}{K_{a,R1}} = \frac{[CH_3COCOO^-(g)](1+x)[H_2O(g)]}{[CH_3COCOOH(g)][HO^-_{interface}(g)]}$$
$$\times \frac{[CH_3COOH(g)][HO^-_{interface}(g)]}{[CH_3COO^-(g)][H_2O(g)]} \tag{7}$$

where the factor $(1 + x)$ is included to account for the larger cluster. A simple numerical solution of eq 7, $12.44 = (1 + x)/1$, is obtained by assuming a constant level of $HO^-_{interface}(g)$ at pH = pK$_a$, when both ratios of dissociated to undissociated acid cancel out as they equal 1/2 each, and other processes such as the reversible hydration of the carbonyl group of pyruvic acid, the formation of stabilizing hydrogen bonds with the acid−base pair, and so forth demand x H$_2$O(g) molecules more for reaction R2 than acetic acid requires in reaction R1. Thus, close interactions with water clusters are formed by gaseous pyruvic acid and the freshly formed pyruvate during and after proton transfer to $HO^-_{interface}$. These water clusters are about $x = 11$ H$_2$O(g) molecules larger than for acetic acid/acetate.

■ CONCLUSIONS

The different pK$_a$ values for acetic and pyruvic acids on the surface of water relative to the bulk reflect the ability of interfacial water molecules to accept protons at lower pH. The variable pK$_a$ shifts for each acid from the bulk to the surface of water is primarily due to the differential hydration of each

acid−base pair. Pyruvic acid and pyruvate, by having a carbonyl group, may interact with a larger number of interfacial water molecules than acetic acid. Future work should aim to optimize the minimum energy orientation of pyruvic acid and pyruvate at the air−water interface. Also needed is an evaluation of the difference in the free energy of hydration of both acids at the interface. Calculations should estimate hydration energies and entropies to be matched with our experimental pK_a measurements.

This work has explored for the first time the transfer of protons to the air−water interface by acetic acid and pyruvic acid. A value of 0.06 has been estimated for the reactive uptake coefficient of gaseous pyruvic acid by water. The new understanding gained by contrasting the role of carboxylic acids "in" water and "on" the surface of water is of major atmospheric relevance.[44] Under environmentally relevant conditions of atmospheric particles with pH < 5, both acetic and pyruvic acids spontaneously transfer protons to the interfacial dangling basic groups, HO$^-_{interface}$, of water. Remarkably, the size of the water cluster involved in the previous uptake is larger than for acetic acid. The previous observation implies that the accommodation of pyruvic acid at the air−water interface must involve the participation of a carbonyl moiety (which undergoes reversible hydration) in addition to the −COOH group. For example, as the pH of the air−water interface drops when any carboxylic acid yields its proton, the molecules of pyruvic acid available in these nanoscopic layers can become more photoreactive as the undissociated fraction grows. Therefore, the photochemical formation of reactive ketyl and acetyl radicals from the λ > 295 nm photolysis of pyruvic acid is favored,[16,17] contributing to the environmental processing of lipids[19] and as a potential source of complex secondary organic aerosol generation.[16]

AUTHOR INFORMATION

Corresponding Author

*E-mail: marcelo.guzman@uky.edu. Phone: (859)323-2892.

ORCID

Agustín J. Colussi: 0000-0002-3400-4101

Marcelo I. Guzman: 0000-0002-6730-7766

Notes

The authors declare no competing financial interest.

ACKNOWLEDGMENTS

ABBREVIATIONS

Da, dalton; ESI-MS, electrospray ionization mass spectrometry; HO$^-_{interface}$, interfacial dangling basic groups of water; I, ion count; K_a, acid dissociation constant; K_H, Henry's law constant; K_{Hyd}, equilibrium of hydration constant; m/z, mass-to-charge ratio; n, number density; OESI-MS, online electrospray ionization mass spectrometry; SIM, single ion monitoring; $S_{HO^-_{interface}}$, surface density of HO$^-_{interface}$; q, surface charge density; α, dissociation fraction; γ_{AA}, reactive uptake coefficient of acetic acid by water; γ_{PA}, reactive uptake coefficient of pyruvic acid by water; v_{AA}, mean thermal velocity of acetic acid; v_{PA}, mean thermal velocity of pyruvic acid; τ_c, contact time

REFERENCES

(1) Mishra, H.; Enami, S.; Nielsen, R. J.; Stewart, L. A.; Hoffmann, M. R.; Goddard, W. A.; Colussi, A. J. Bronsted basicity of the air-water interface. *Proc. Natl. Acad. Sci. U.S.A.* **2012**, *109*, 18679−18683.

(2) Parashar, S.; Lesnicki, D.; Sulpizi, M. Increased acid dissociation at the quartz/water interface. *J. Phys. Chem. Lett.* **2018**, *9*, 2186−2189.

(3) Cheng, J.; Psillakis, E.; Hoffmann, M. R.; Colussi, A. J. Acid dissociation versus molecular association of perfluoroalkyl oxoacids: Environmental implications. *J. Phys. Chem. A* **2009**, *113*, 8152−8156.

(4) Wellen, B. A.; Lach, E. A.; Allen, H. C. Surface pK_a of octanoic, nonanoic, and decanoic fatty acids at the air−water interface: applications to atmospheric aerosol chemistry. *Phys. Chem. Chem. Phys.* **2017**, *19*, 26551−26558.

(5) Balzan, R.; Fernandes, L.; Pidial, L.; Comment, A.; Tavitian, B.; Vasos, P. R. Pyruvate cellular uptake and enzymatic conversion probed by dissolution DNP-NMR: the impact of overexpressed membrane transporters. *Magn. Reson. Chem.* **2017**, *55*, 579−583.

(6) Guzman, M. I. Abiotic photosynthesis: from prebiotic chemistry to metabolism. In *Origins of Life: The Primal Self-Organization*; Egel, R., Lankenau, D.-H., Mulkidjanian, A. Y., Eds.; Springer Berlin Heidelberg, 2011; pp 85−105.

(7) Guzman, M. I.; Martin, S. T. Oxaloacetate-to-malate conversion by mineral photoelectrochemistry: implications for the viability of the reductive tricarboxylic acid cycle in prebiotic chemistry. *Int. J. Astrobiol.* **2008**, *7*, 271−278.

(8) Rapf, R. J.; Vaida, V. Sunlight as an energetic driver in the synthesis of molecules necessary for life. *Phys. Chem. Chem. Phys.* **2016**, *18*, 20067−20084.

(9) Hazen, R. M.; Deamer, D. W. Hydrothermal reactions of pyruvic acid: Synthesis, selection, and self-assembly of amphiphilic molecules. *Origins Life Evol. Biospheres* **2007**, *37*, 143−152.

(10) Fu, P.; Kawamura, K.; Usukura, K.; Miura, K. Dicarboxylic acids, ketocarboxylic acids and glyoxal in the marine aerosols collected during a round-the-world cruise. *Mar. Chem.* **2013**, *148*, 22−32.

(11) Kawamura, K.; Tachibana, E.; Okuzawa, K.; Aggarwal, S. G.; Kanaya, Y.; Wang, Z. F. High abundances of water-soluble dicarboxylic acids, ketocarboxylic acids and α-dicarbonyls in the mountaintop aerosols over the North China Plain during wheat burning season. *Atmos. Chem. Phys.* **2013**, *13*, 8285−8302.

(12) Mkoma, S. L.; Kawamura, K. Molecular composition of dicarboxylic acids, ketocarboxylic acids, α-dicarbonyls and fatty acids in atmospheric aerosols from Tanzania, East Africa during wet and dry seasons. *Atmos. Chem. Phys.* **2013**, *13*, 2235−2251.

(13) Carlton, A. G.; Turpin, B. J.; Lim, H.-J.; Altieri, K. E.; Seitzinger, S. Link between isoprene and secondary organic aerosol (SOA): Pyruvic acid oxidation yields low volatility organic acids in clouds. *Geophys. Res. Lett.* **2006**, *33*, L06822.

(14) Pillar, E. A.; Guzman, M. I. Oxidation of Substituted Catechols at the Air−Water Interface: Production of Carboxylic Acids, Quinones, and Polyphenols. *Environ. Sci. Technol.* **2017**, *51*, 4951−4959.

(15) Herrmann, H.; Schaefer, T.; Tilgner, A.; Styler, S. A.; Weller, C.; Teich, M.; Otto, T. Tropospheric aqueous-phase chemistry: Kinetics, mechanisms, and its coupling to a changing gas phase. *Chem. Rev.* **2015**, *115*, 4259−4334.

(16) Eugene, A. J.; Guzman, M. I. Reactivity of ketyl and acetyl radicals from direct solar actinic photolysis of aqueous pyruvic acid. *J. Phys. Chem. A* **2017**, *121*, 2924−2935.

(17) Eugene, A. J.; Guzman, M. I. Reply to "Comment on Reactivity of Ketyl and Acetyl Radicals from Direct Solar Actinic Photolysis of Aqueous Pyruvic Acid". *J. Phys. Chem. A* **2017**, *121*, 8741−8744.

(18) Eugene, A. J.; Xia, S.-S.; Guzman, M. I. Negative production of acetoin in the photochemistry of aqueous pyruvic acid. *Proc. Natl. Acad. Sci. U.S.A.* **2013**, *110*, E4274−E4275.

(19) Rapf, R. J.; Perkins, R. J.; Dooley, M. R.; Kroll, J. A.; Carpenter, B. K.; Vaida, V. Environmental processing of lipids driven by aqueous photochemistry of α-keto acids. *ACS Cent. Sci.* **2018**, *4*, 624−630.

(20) Epstein, S. A.; Tapavicza, E.; Furche, F.; Nizkorodov, S. A. Direct photolysis of carbonyl compounds dissolved in cloud and fog droplets. *Atmos. Chem. Phys.* **2013**, *13*, 9461−9477.

(21) Horowitz, A.; Meller, R.; Moortgat, G. K. The UV−VIS absorption cross sections of the α-dicarbonyl compounds: pyruvic acid, biacetyl and glyoxal. *J. Photochem. Photobiol., A* **2001**, *146*, 19−27.

(22) Saxena, P.; Hildemann, L. M. Water-soluble organics in atmospheric particles: A critical review of the literature and application of thermodynamics to identify candidate compounds. *J. Atmos. Chem.* **1996**, *24*, 57−109.

(23) Physical Constants of Organic Compunds. In *CRC Handbook of Chemistry and Physics*, 97th ed.; Haynes, W. M., Ed.; CRC Press/ Taylor & Francis: Boca Raton, FL, internet version, 2017.

(24) Guzmán, M. I.; Hildebrandt, L.; Colussi, A. J.; Hoffmann, M. R. Cooperative hydration of pyruvic acid in ice. *J. Am. Chem. Soc.* **2006**, *128*, 10621−10624.

(25) Leermakers, P. A.; Vesley, G. F. The Photochemistry of α-Keto Acids and α-Keto Esters. I. Photolysis of Pyruvic Acid and Benzoylformic Acid. *J. Am. Chem. Soc.* **1963**, *85*, 3776−3779.

(26) Fischer, M.; Warneck, P. The dissociation constant of pyruvic acid: Determination by spectrophotometric measurements. *Ber. Bunsen-Ges.* **1991**, *95*, 523−527.

(27) Guzman, M. I.; Athalye, R. R.; Rodriguez, J. M. Concentration effects and ion properties controlling the fractionation of halides during aerosol formation. *J. Phys. Chem. A* **2012**, *116*, 5428−5435.

(28) Pillar, E. A.; Camm, R. C.; Guzman, M. I. Catechol oxidation by ozone and hydroxyl radicals at the air−water interface. *Environ. Sci. Technol.* **2014**, *48*, 14352−14360.

(29) Pillar, E. A.; Guzman, M. I.; Rodriguez, J. M. Conversion of iodide to hypoiodous acid and iodine in aqueous microdroplets exposed to ozone. *Environ. Sci. Technol.* **2013**, *47*, 10971−10979.

(30) Pillar, E. A.; Zhou, R.; Guzman, M. I. Heterogeneous oxidation of catechol. *J. Phys. Chem. A* **2015**, *119*, 10349−10359.

(31) Acree, W. E., Jr.; Chickos, J. S. Phase Transition Enthalpy Measurements of Organic and Organometallic Compounds. In *NIST Chemistry WebBook, NIST Standard Reference Database Number 69 [Online]*; Linstrom, P. J., Mallard, W. G., Eds.; National Institute of Standards and Technology: Gaithersburg MD (accessed Dec 19, 2017).

(32) Bu, W.; Vaknin, D.; Travesset, A. How Accurate Is Poisson−Boltzmann Theory for Monovalent Ions near Highly Charged Interfaces? *Langmuir* **2006**, *22*, 5673−5681.

(33) Beattie, J. K.; Djerdjev, A. M.; Warr, G. G. The surface of neat water is basic. *Faraday Discuss.* **2009**, *141*, 31−39.

(34) Hu, J. H.; Shorter, J. A.; Davidovits, P.; Worsnop, D. R.; Zahniser, M. S.; Kolb, C. E. Uptake of gas-phase halogenated acetic acid molecules by water surfaces. *J. Phys. Chem.* **1993**, *97*, 11037−11042.

(35) Cheng, J.; Hoffmann, M. R.; Colussi, A. J. Anion Fractionation and Reactivity at Air/Water:Methanol Interfaces. Implications for the Origin of Hofmeister Effects. *J. Phys. Chem. B* **2008**, *112*, 7157−7161.

(36) Enami, S.; Fujii, T.; Sakamoto, Y.; Hama, T.; Kajii, Y. Carboxylate Ion Availability at the Air−Water Interface. *J. Phys. Chem. A* **2016**, *120*, 9224−9234.

(37) Marinova, K. G.; Alargova, R. G.; Denkov, N. D.; Velev, O. D.; Petsev, D. N.; Ivanov, I. B.; Borwankar, R. P. Charging of Oil−Water Interfaces Due to Spontaneous Adsorption of Hydroxyl Ions. *Langmuir* **1996**, *12*, 2045−2051.

(38) Johnson, C. M.; Tyrode, E.; Baldelli, S.; Rutland, M. W.; Leygraf, C. A Vibrational Sum Frequency Spectroscopy Study of the Liquid−Gas Interface of Acetic Acid−Water Mixtures: 1. Surface Speciation. *J. Phys. Chem. B* **2005**, *109*, 321−328.

(39) Kim, G.; Gurau, M.; Kim, J.; Cremer, P. S. Investigations of lysozyme adsorption at the air/water and quartz/water interfaces by

vibrational sum frequency spectroscopy. *Langmuir* **2002**, *18*, 2807−2811.

(40) Tyrode, E.; Johnson, C. M.; Baldelli, S.; Leygraf, C.; Rutland, M. W. A Vibrational Sum Frequency Spectroscopy Study of the Liquid−Gas Interface of Acetic Acid−Water Mixtures: 2. Orientation Analysis. *J. Phys. Chem. B* **2005**, *109*, 329−341.

(41) Houriez, C.; Meot-Ner, M.; Masella, M. Simulated solvation of organic ions II: Study of linear alkylated carboxylate ions in water nanodrops and in liquid water. Propensity for air/water interface and convergence to bulk solvation properties. *J. Phys. Chem. B* **2015**, *119*, 12094−12107.

(42) Ottosson, N.; Wernersson, E.; Söderström, J.; Pokapanich, W.; Kaufmann, S.; Svensson, S.; Persson, I.; Öhrwall, G.; Björneholm, O. The protonation state of small carboxylic acids at the water surface from photoelectron spectroscopy. *Phys. Chem. Chem. Phys.* **2011**, *13*, 12261−12267.

(43) Richard Drees, L.; Wilding, L. P.; Smeck, N. E.; Senkayi, A. L. Silica in Soils: Quartz and Disordered Silica Polymorphs. In *Minerals in Soil Environments*; Dixon, J. B., Weed, S. B., Eds.; Soil Science Society of America: Madison, WI, 1989; pp 913−974.

(44) Finlayson-Pitts, B. J. Reactions at surfaces in the atmosphere: integration of experiments and theory as necessary (but not necessarily sufficient) for predicting the physical chemistry of aerosols. *Phys. Chem. Chem. Phys.* **2009**, *11*, 7760−7779.

■ NOTE ADDED AFTER ASAP PUBLICATION

This paper was published ASAP on July 23, 2018, with errors in the text. The corrected version was reposted on July 24, 2018.